ACCELERATOR DIVISION

Insertion Devices Section

ALBA Project Document No.	*EDMS Document No.*	*Created:* 31.07.06	*Page:* 1/19
AAD-SR-ID-AN-0149		*Modified:*	*Rev. No.:* Draft 0.0

Determination of main parameters of a wiggler feeding the EXAFS beamline at ALBA

Abstract

In this document we present the determination of period and K-value, as well as the technology, for the wiggler to feed the EXAFS beamline

Prepared by:	*Checked by:*	*Approved by:*
J. Campmany		
Authorship:		

Distribution list:

Anybody who asked

Table of Contents

Record of Changes

Rev. No.	*Date*	*Pages*	*Description of changes*

References

[1] K. Klementiev, *Considerations related to the wiggler parameters for EXAFS beamline*, pivate communication 12/05/06.

[2] J. Campmany, *Optimization of a wiggler as a source for EXAFS beamline – I*, AAD-SR-ID-AN-0147.

[3] J. Campmany, *Optimization of a wiggler as a source for EXAFS beamline – II*, AAD-SR-ID-AN-0148.

[4] M. Sanchez del Rio, R. J. Dejus, "XOP: A Multiplatform Graphical User Interface for Synchrotron Radiation Spectral and Optics Calculations," SPIE Proc., 3152 (1997) 148.

[5] P. Elleaume, J. Chavanne, Bart Faatz, *Design considerations for a 1As SASE undulator,* Nuclear Instruments and Methods in Physics Research A 455 (2000) 503-523.

1. Introduction

In this paper we will make a survey of possible insertion devices for feeding the ALBA EXAFS beamline. Several lengths and periods are explored. We look for the "optimum" device with respect some types of experiments and several electron currents in the accelerator.

In following sections within this chapter, we present the experimental scenarios for this beamline, which have been used to optimize the insertion device. Data to define these scenarios have been given by Experiments Division [1]. Several approaches have been done previously [2, 3].

1.1. Type of experiments and usage of emission spectrum.

The EXAFS experiments are made in well defined energy ranges. For each range, a configuration of mirrors and filters is used. We detail these configurations in Table 1 below.

Range	Energies	Filters	Mirrors
Low energy	0 – 7 keV	Filter can be used to screen high energies	Mirror do not transmit energies above 7 keV
Medium energy	7 – 20 keV	Filter is used to screen energies below 7 keV	Mirror do not transmit energies above 20 keV
High energy	20 – INF keV	Filter is used to screen energies below 20 keV	No mirror is used

Table 1. Experimental scenarios for EXAFS beamline

1.2. Apertures

In the vertical plane, due to the availability of space and the position of the first mirror, the maximum available aperture is 250 μrad.

In the horizontal plane, the aperture can be chosen fron 1.5 mrad to 2.5 mrad. In order to carry out the calculations for optimizing the insertion device, we will only consider the 1.5 mrad aperture. This is because the beamline should provide a high photon flux at high energies, as it will be explained in section 2.4.

1.3. Scenarios regarding currents in the ring.

The nominal current in the accelerator is 250 mA. However, the dimensioning of absorbers and front ends have been done considering an electron current of 400 mA. This is the current that should be used to calculate the maximum power emitted by the insertion device.

Moreover, during the initial commissioning period, the current in the machine is not expected to be higher than 100 mA.

All these scenarios should be taken into account when doing the optimization.

1.4. Gap adaptability

In order to have big flexibility for the beam line operation, it has been requested by Experiments Division to provide an insertion device with variable gap. Even it will be used as a wiggler, the possibility to change the gap will be used to adapt the device to different scenarios of current in the accelerator.

2. Constraints coming from power delivered to beamline

2.1. Maximum power in the front end.

The maximum power that the Front End can tolerate is 20 kW. The power is given by:

$$P_{TOT} = 0.6328 \cdot I \cdot E^2 \cdot L \cdot B^2$$

being I the electron intensity in [A], E the electron energy in [GeV], L the length of the device in [m] and B the maximum magnetic field in the axis of the device in [T].

In general, increasing the K value of the device (and thus the maximum B field), the power deposited by the wiggler into the beamline also increases. So, the constraint in the maximum power allowed for the device translates into a constraint in the maximum K value the insertion device can have. It is important to take into account this constraint because, for a given machine (I, E) and a given length of the device, it introduces a limitation in the maximum magnetic field in the axis of the device, and thus the K value of the undulator.

2.2. Maximum power in the mirror

For the optimization we have carried out, we have considered as a constraint that the maximum power that can be absorbed by the mirror is around 1 kW. In fact, this is not the most severe constraint, but it should be taken into account. In order to do this, we have approximated the effect of the mirror into the spectral density of photon flux to a step function:

- 1 for energies below 7 keV (or 20 keV)
- 0 for energies above 7 keV (or 20 keV).

We used this to compute the power deposited on the mirror and that reflected to the monochromator.

2.3. Maximum power in the monochromator

The maximum power allowed to enter the monochromator is 700 W. This is the most severe limitation in most of the cases. It impinges on the maximum B, and thus on the K value of the device. This limitation has to be applied to each of the spectrum ranges defined in Table 1 above.

In order to carry out the optimization, for each possible insertion device (i. e. a pair of values for period length and device length) we have determined the maximum K achievable as that delivering up to 700 W in at least one of the operation ranges: 0-7 keV, 7-20 keV, 20-INF keV.

Although there is not an easy analytical expression relating the power through a given aperture and in an energy range, the constraint on the power delivered to the monochromator determines a K maximum value for a given pair of period and device lengths.

2.4. Optimization aperture.

Whilst vertical aperture have requested to be 0.25 mrad, the horizontal aperture in principle can have a range between 1.5 and 2.5 mrad.

Because of power limitations described above, for each device and period lengths it exists a maximum K value that is feasible from the point of view of power into beamline.

It is well known that, for each period length, K value has a direct impact on the critical energy of the spectrum produced by the wiggler, being the relationship between the maximum field in the axis of the device B_0 in [T] and the period length λ_u in [mm] and the K value:

$$K = 0.0934 \cdot \lambda_u \cdot B_0$$

The relationship between B_0 and the critical energy of the wiggler emission spectrum on axis is:

$$\varepsilon_0 = 0.665 \cdot E^2 \cdot B_0$$

where the electron energy E is expressed in [GeV] and the maximum magnetic field B_0 in [T]. Thus, the constraints on maximum power described above have an impact in the photon flux density spectrum, through the maximum critical energy achievable for each device.

It is straightforward that for small slit apertures, the power deposited into beamline is also small, and thus the maximum allowed K value (or B_0) is high. This implies that the emission spectrum is displaced towards high energies. So, because experimental reasons push to have a beamline with good performance at high energies (~34 keV) without loosing efficiency at low energies (~2.4 keV), we have used in the optimization a small value for the horizontal aperture: 1.5 mrad.

It should be understood that this horizontal aperture is only considered for optimization. When operating at low energies, horizontal aperture can be opened up to reach the limit of 700 W delivered to the beamline.

3. Parameter exploration and results

We have computed the maximum photon flux given by different insertion devices at two reference energies: 2.4 keV and 34 keV. We have considered several period lengths for a number of device lengths (1 m, 1.5 m, 2 m) for 400 mA of current scenario. Results have been obtained with WS code in XOP package [1] and are shown in Tables 2 to 4.

Length 1000 mm, current 400 mA													
Period (mm)	**30**	**40**	**50**	**60**	**70**	**80**	**90**	**100**	**110**	**120**	**130**	**140**	**150**
Number of periods N	33	25	20	16	14	12	11	10	9	8	7	7	6
H Slit (mrad)	1.5	1.5	1.5	1.5	1.5	1.5	1.5	1.5	1.5	1.5	1.5	1.5	1.5
Power through slit 0-7 keV (W)	700.1	700	700.1	700	640.1	542.4	491.2	437.8	380.9	317.2	264.2	264.2	219.6
Power through slit 7-20 keV (W)	351.2	347.3	348.4	414.1	700.1	700	700	700	700	700	644.6	644.6	564.8
Power through slit 20-INF keV (W)	27.6	26.8	27	39.6	158.7	209.8	250.3	310	406.7	600.6	700	700	700
Power through slit 7 - INF (W)	379	374	375	454	859	910	950	1010	1107	1301	1345	1345	1265
Power through slit 0-20 keV (W)	1051	1047	1049	1114	1340	1242	1191	1138	1081	1017	909	909	784
Power through slit (W)	1079	1074	1076	1154	1499	1452	1442	1448	1488	1618	1609	1609	1484
K maximum (total power)	8.302	11.070	13.837	16.605	19.372	22.139	24.907	27.674	30.442	33.209	35.977	38.744	41.512
K	2.254	2.985	3.735	4.812	7.406	9.328	11.222	13.653	17.036	22.625	27.797	29.918	34.475
Flux @ 2.4 keV (Ph/s/0.1%BW)	7.74E14	7.74E14	7.75E14	7.55E14	6.28E14	5.01E14	4.45E14	3.88E14	3.29E14	2.64E14	2.16E14	2.16E14	1.78E14
Flux @ 34 keV (Ph/s/0.1%BW)	1.98E12	1.89E12	1.91E12	3.19E12	1.25E13	2.89E13	3.66E13	4.82E13	6.69E13	1.02E14	1.18E14	1.18E14	1.17E14

***Table 2**. Photon fluxes at low and high energies (green cells) and maximum K values (yellow cells) for a number of wigglers 1 m long and a number of periods. Blue cells mark the limiting constraint.*

Length 1500 mm, current 400 mA													
Period (mm)	60	70	80	90	100	110	120	130	140	150	160	170	180
Number of periods N	25	21	18	16	15	13	12	11	10	10	9	8	8
H Slit (mrad)	1.5	1.5	1.5	1.5	1.5	1.5	1.5	1.5	1.5	1.5	1.5	1.5	1.5
Power through slit 0-7 keV (W)	700	700.3	700	700	688	592.3	542.6	491.3	437.8	437.8	380.9	317.2	317.2
Power through slit 7-20 keV (W)	192	198.8	213.4	504	700	700	700	700	700	700	700	700	700
Power through slit 20-INF keV (W)	5.5	6	7.1	45.8	138.2	178.8	208.7	249.8	309.7	309.8	406.6	600.6	600.2
Power through slit 7 - INF (W)	198	205	221	550	838	879	909	950	1010	1010	1107	1301	1300
Power through slit 0-20 keV (W)	892	899	913	1204	1388	1292	1243	1191	1138	1138	1081	1017	1017
Power through slit (W)	898	905	921	1250	1526	1471	1451	1441	1448	1448	1488	1618	1617
K maximum (total power)	13.558	15.817	18.077	20.336	22.596	24.856	27.115	29.375	31.634	33.894	36.154	38.413	40.673
K	3.347	3.963	4.643	6.162	9.768	11.812	13.685	15.982	18.945	20.277	24.63	31.95	33.81
Flux @ 2.4 keV (Ph/s/0.1%BW)	8.39E14	8.36E14	8.32E14	7.70E14	6.65E14	5.57E14	5.01E14	4.45E14	3.88E14	3.88E14	3.29E14	2.64E14	2.64E14
Flux @ 34 keV (Ph/s/0.1%BW)	1.93E11	2.21E11	2.79E11	1.31E12	1.59E13	2.31E13	2.87E13	3.65E13	4.82E13	4.82E13	6.69E13	1.02E14	1.02E14

***Table 3**. Photon fluxes at low and high energies (green cells) and maximum K values (yellow cells) for a number of wigglers 1.5 m long and a number of periods. Blue cells mark the limiting constraint.*

Length 2000 mm, current 400 mA													
Period (mm)	**70**	**80**	**90**	**100**	**110**	**120**	**130**	**140**	**150**	**160**	**170**	**180**	**190**
Number of periods N	28	25	22	20	18	16	15	14	13	12	11	11	10
H Slit (mrad)	1.5	1.5	1.5	1.5	1.5	1.5	1.5	1.5	1.5	1.5	1.5	1.5	1.5
Power through slit 0-7 keV (W)	700.1	700.1	700.1	700.3	700.1	700	688.2	640.8	592.3	542.6	491.3	491.3	437.8
Power through slit 7-20 keV (W)	124.5	120.6	122.8	128	177.7	339.7	700	700	700	700	700	700	700
Power through slit 20-INF keV (W)	1.7	1.6	1.7	1.8	3.7	19.3	137.6	155.6	178.5	208.5	249.7	249.7	309.6
Power through slit 7 - INF (W)	126	122	125	130	181	359	838	856	879	909	950	950	1010
Power through slit 0-20 keV (W)	825	821	823	828	878	1040	1388	1341	1292	1243	1191	1191	1138
Power through slit (W)	826	822	825	830	882	1059	1526	1496	1471	1451	1441	1441	1447
K maximum (total power)	13.698	15.655	17.612	19.569	21.526	23.482	25.439	27.396	29.353	31.310	33.267	35.224	37.181
K	3.273	3.695	4.184	4.684	5.634	7.796	12.514	14.095	15.927	18.105	20.788	21.992	25.603
Flux @ 2.4 keV (Ph/s/0.1%BW)	8.69E14	8.71E14	8.71E14	8.78E14	8.50E14	7.73E14	6.65E14	6.11E14	5.57E14	5.01E14	4.45E14	4.45E14	3.88E14
Flux @ 34 keV (Ph/s/0.1%BW)	3.39E10	2.97E10	3.19E10	3.53E10	1.00E11	1.06E12	1.58E13	1.89E13	2.30E13	2.86E13	3.65E13	3.65E13	4.82E13

Table 4*. Photon fluxes at low and high energies (green cells) and maximum K values (yellow cells) for a number of wigglers 1 m long and a number of periods. Blue cells mark the limiting constraint.*

From tables above it can be seen that the main limitation to have high K values and thus high photon fluxes at high energies, it is not the maximum power to the front end, but the power to the monochromator. This is the main limitation.

It can also be seen that for different periods, the limitation happens at different energy ranges: at low periods, the main limitation comes from power delivered low energies, whilst for larger periods the limitation happens at medium or high energy ranges. It can also be observed that short devices give a better performance than long devices at high energies, whilst the long devices are more suitable for experiments at low energy ranges. This can be seen in Figure 1 below.

The results show a saturation of the flux for high periods, coming from constraint of maximum power tolerable in the range 20 keV to infinite. In order to achieve this maximum flux, a minimum period of 130 mm should be used. The drawback of this election is that, at low energies, higher the period, lower the flux, at least in the conditions fixed for the optimization (1.5 mrad of horizontal aperture). At low energies the aperture of the horizontal slit can be opened up to 2.5 mrad, but the gain in flux is not big, as we will see below.

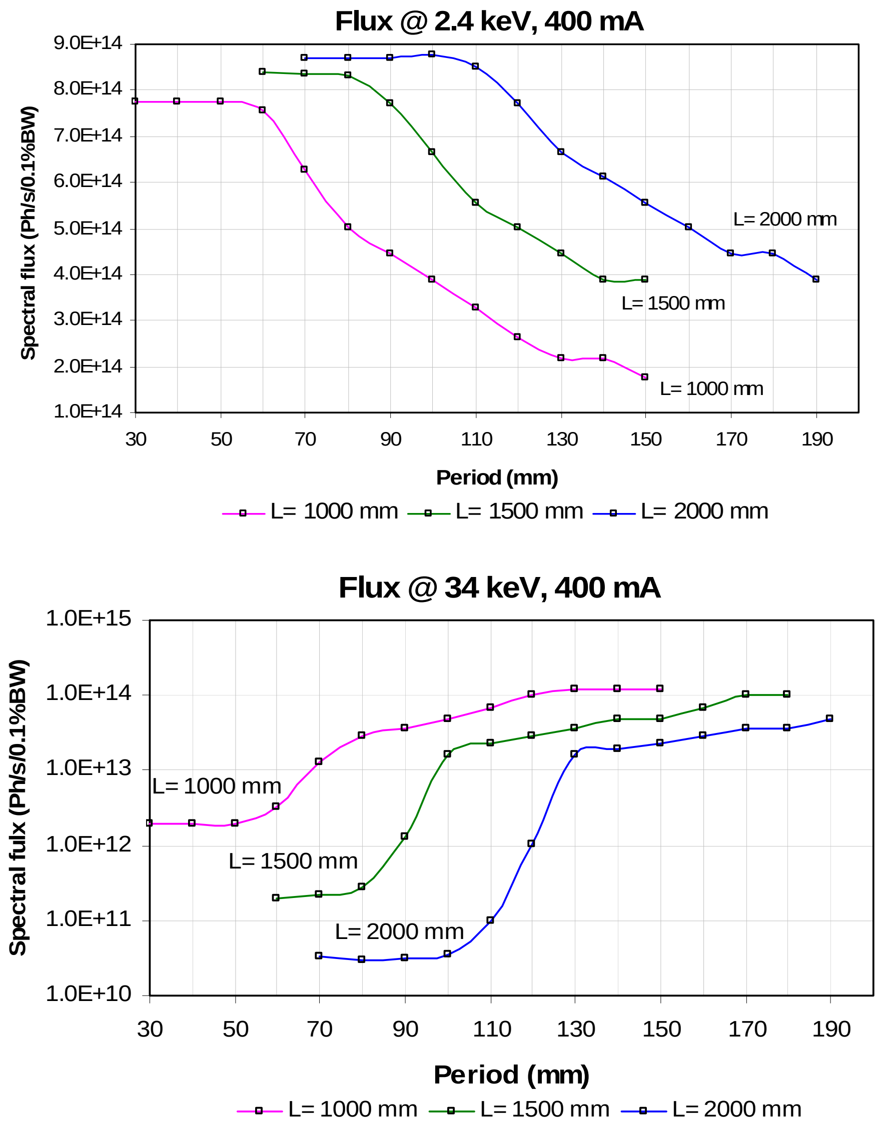

Figure 1. *Flux at 2.4 keV (top) and 34 keV(bottom) with an electron current of 400 mA for a number of devices. All constraints specified in chapter 2 have been introduced.*

A reasonable balance between performances at low and high energies can be found between the period ranges shown in Table 5 below:

Length of the device	Range of optimum periods
1000 mm	50 – 130 mm
1500 mm	80 – 170 mm
2000 mm	100 – >190 mm

Table 5. *Range of optimum periods for the EXAFS wiggler*

In order to go further with the optimization, we should consider other electron current scenarios that may take place at ALBA ring. We have repeated the exploration for a current of 250 mA, as given in Tables 6 to 8.

Length 1000 mm, current 250 mA													
Period (mm)	10	20	30	40	50	60	70	80	90	100	110	120	130
Number of periods N	100	50	33	25	20	16	14	12	11	10	9	8	7
H Slit (mrad)	1.5	1.5	1.5	1.5	1.5	1.5	1.5	1.5	1.5	1.5	1.5	1.5	1.5
Power through slit 0-7 keV (W)	700	700.1	700	698.8	565.8	437.5	365.8	286.7	258.6	230.7	203.1	175.8	148.9
Power through slit 7-20 keV (W)	688	661.2	675.8	700.2	700.1	700	700	683	634.9	585.1	533.7	480.2	424.6
Power through slit 20-INF keV (W)	159.4	148.2	156.1	166.1	202.6	312.4	442.3	700	700	700	700	700	700
Power through slit 7 - INF (W)	847	809	832	866	903	1012	1142	1383	1335	1285	1234	1180	1125
Power through slit 0-20 keV (W)	1388	1361	1376	1399	1266	1138	1066	970	894	816	737	656	574
Power through slit (W)	1547	1510	1532	1565	1469	1450	1508	1670	1594	1516	1437	1356	1274
K maximum (total power)	2.767	5.535	8.302	11.070	13.837	16.605	19.372	22.139	24.907	27.674	30.442	33.209	35.977
K	1.136	2.237	3.4	4.584	6.032	8.459	11.466	16.696	19.493	22.613	26.153	30.257	35.15
Flux @ 2.4 keV (Ph/s/0.1%BW)	6.92E14	6.99E14	6.93E14	6.88E14	5.28E14	3.88E14	3.13E14	2.35E14	2.11E14	1.87E14	1.64E14	1.40E14	1.18E14
Flux @ 34 keV (Ph/s/0.1%BW)	2.03E13	1.86E13	1.99E13	2.14E13	2.77E13	4.87E13	7.36E13	1.19E14	1.18E14	1.17E14	1.16E14	1.14E14	1.11E14

Table 6. *Photon fluxes at low and high energies (green cells) and maximum K values (yellow cells) for a number of wigglers 1 m long and a number of periods. Blue cells mark the limiting constraint.*

Length 1500 mm, current 250 mA												
Period (mm)	20	30	40	50	60	70	80	90	100	110	120	130
Number of periods N	75	50	37	30	25	21	18	16	15	13	12	11
H Slit (mrad)	1.5	1.5	1.5	1.5	1.5	1.5	1.5	1.5	1.5	1.5	1.5	1.5
Power through slit 0-7 keV (W)	699.9	700	700.1	700	700	597.9	504.2	437.8	402.8	325.8	286.7	258.6
Power through slit 7-20 keV (W)	388	383	391.5	385.8	480.9	700	700	700	700	700	683.1	634.9
Power through slit 20-INF keV (W)	35.4	34.5	36.5	35	55.7	178	239.1	310.2	364	565.4	700	700
Power through slit 7 - INF (W)	423	418	428	421	537	878	939	1010	1064	1265	1383	1335
Power through slit 0-20 keV (W)	1088	1083	1092	1086	1181	1298	1204	1138	1103	1026	970	894
Power through slit (W)	1123	1118	1128	1121	1237	1476	1443	1448	1467	1591	1670	1594
K maximum (total power)	4.519	6.779	9.038	11.298	13.558	15.817	18.077	20.336	22.596	24.856	27.115	29.375
K	1.58	2.36	3.184	3.943	5.13	7.734	9.847	12.34	14.717	20.12	24.882	28.03
Flux @ 2.4 keV (Ph/s/0.1%BW)	7.66E14	7.58E14	7.64E14	7.66E14	7.33E14	5.63E14	4.59E14	3.88E14	3.51E14	2.73E14	2.35E14	2.11E14
Flux @ 34 keV (Ph/s/0.1%BW)	2.78E12	2.69E12	2.91E12	2.74E12	5.00E12	2.30E13	3.45E13	4.83E13	5.87E13	9.61E13	1.19E14	1.18E14

Table 7. *Photon fluxes at low and high energies (green cells) and maximum K values (yellow cells) for a number of wigglers 1.5 m long and a number of periods. Blue cells mark the limiting constraint.*

Length 2000 mm, current 250 mA										
Period (mm)	50	60	70	80	90	100	110	120	130	140
Number of periods N	40	33	28	25	22	20	18	16	15	14
H Slit (mrad)	1.5	1.5	1.5	1.5	1.5	1.5	1.5	1.5	1.5	1.5
Power through slit 0-7 keV (W)	700	700.2	700.1	700	628.6	567.6	504.3	437.8	402.8	365.9
Power through slit 7-20 keV (W)	251.4	256.1	264.8	433.7	700	700	700	700	700	700
Power through slit 20-INF keV (W)	11.4	11.9	35.1	38.9	161.7	192.9	238.3	309.8	364	441.6
Power through slit 7 - INF (W)	263	268	300	473	862	893	938	1010	1064	1142
Power through slit 0-20 keV (W)	951	956	965	1134	1329	1268	1204	1138	1103	1066
Power through slit (W)	963	968	1000	1173	1490	1461	1443	1448	1467	1508
K maximum (total power)	9.784	11.741	13.698	15.655	17.612	19.569	21.526	23.482	25.439	27.396
K	3.161	3.825	4.519	6.14	9.393	11.122	13.314	16.293	19.015	22.49
Flux @ 2.4 keV (Ph/s/0.1%BW)	8.11E14	8.08E14	8.08E14	7.43E14	5.98E14	5.29E14	4.59E14	3.88E14	3.51E14	3.13E14
Flux @ 34 keV (Ph/s/0.1%BW)	5.58E11	5.97E11	6.64E11	2.94E12	2.00E13	2.57E13	3.43E13	4.82E13	5.87E13	7.35E13

Table 8. *Photon fluxes at low and high energies (green cells) and maximum K values (yellow cells) for a number of wigglers 1 m long and a number of periods. Blue cells mark the limiting constraint.*

In the case of a current of 250 mA, the parameter exploration gives a similar result as in the case of 400 mA, but with the transitions shifted to lower periods, as shown in Figure 2.

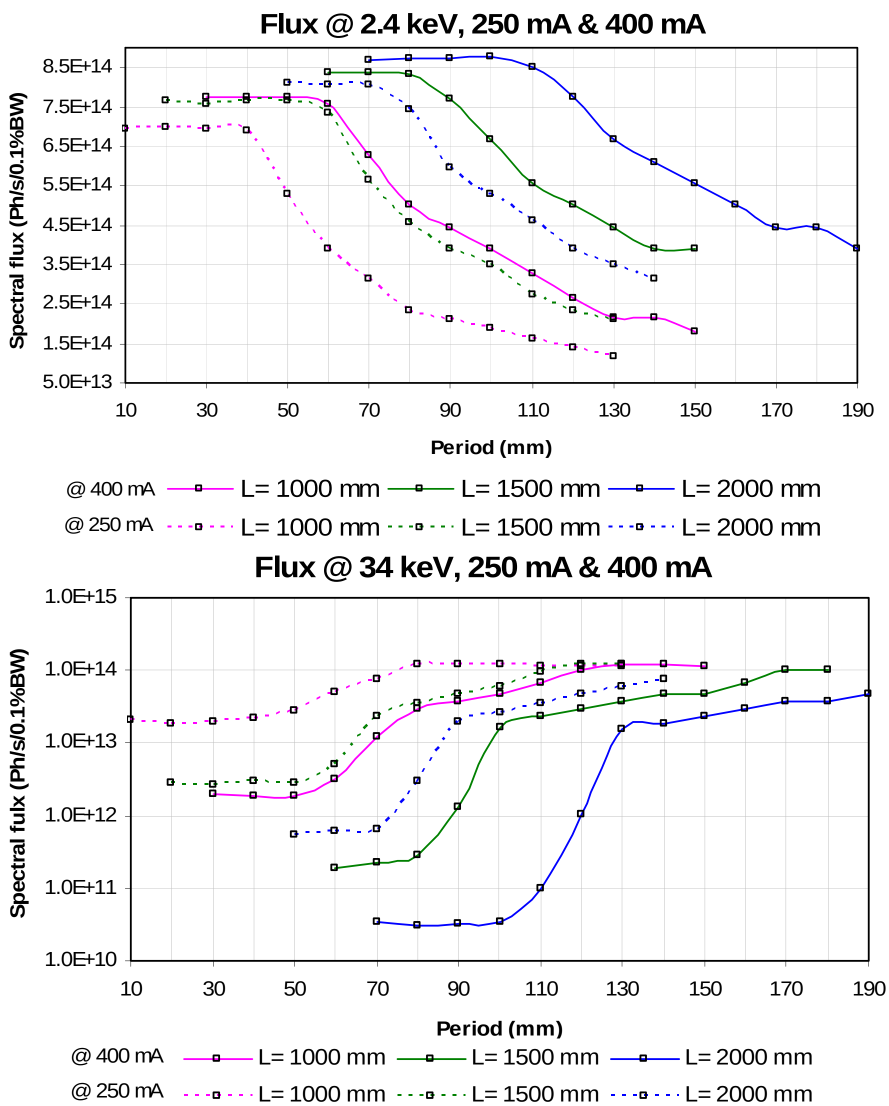

Figure 2. *Flux at 2.4 keV (top) and 34 keV(bottom) for a number of devices. All constraints specified in chapter 2 have been introduced. Currents of 400 and 250 mA have been considered.*

With this additional information we can refine the range of periods giving balanced performance at low and hight energies as shown in table 6:

Length of the device	Range of optimum periods
1000 mm	50 – 80 mm
1500 mm	80 – 110 mm
2000 mm	100 – >150 mm

Table 6. *Range of optimum periods for the EXAFS wiggler at both 250 and 400 mA*

From the exploration presented above it is clear that small device lengths produce better photon fluxes at high energies than long devices. However, in order to choose uniquely the optimum period and length, more constraints should be given.

4. Constraints coming from insertion device technologies

Up to now he have not introduced any assumption referred to ID technology; we have only been dealing with properties of light emitted from the devices.

One first limitation comes from the type of insertion device to be used. Superconducting wigglers provide high magnetic fields (and thus high K values) than conventional wigglers for a given period length. In the case of conventional devices, the limitation in the maximum magnetic field achievable comes basically from the minimum gap the device can reach. So, this is the first issue to be considered.

Second, the available space in the straight section of ALBA ring, along with the future prospectives regarding the distribution of IDs in the ring can also introduce new limitations to the ID length.

Let us see these constraints in detail.

4.1. minimum gap

Regarding to the minimum gap, a magnetic gap of 8.5 mm can be considered if using an Al vacuum chamber APS-type. This chamber can be thinned down to 5 mm internal / 7 mm external height. However, this technological solution will only be considered if the photon flux delivered by the insertion device does not fulfil the requirements of Experiments Division, which is not the case.

Thus, the minimum magnetic gap aperture to be used in the optimization is 12.5 mm, which corresponds to an ESRF-type Al-extruded vacuum chamber with 8 mm internal / 10 mm external height. This chamber is easy to be constructed and CELLS can afford to have some spears.

If considering this constraint, the performance of devices shown in Figure 2 should be corrected specially for low periods: the K value producing the maximum power tolerated by the monochromator is sometimes not achievable by conventional technologies. In Figure 3 we show the calculated reduction in performance. To calculate the maximum K value achievable with a given gap, we have used the empirical expression given in [5]:

$B = 3.694 \cdot \exp\left(-5.068 \frac{g}{\lambda_u} + 1.520 \left(\frac{g}{\lambda_u} \right)^2 \right)$ being «g» the gap and «λ_u» the period of the wiggler.

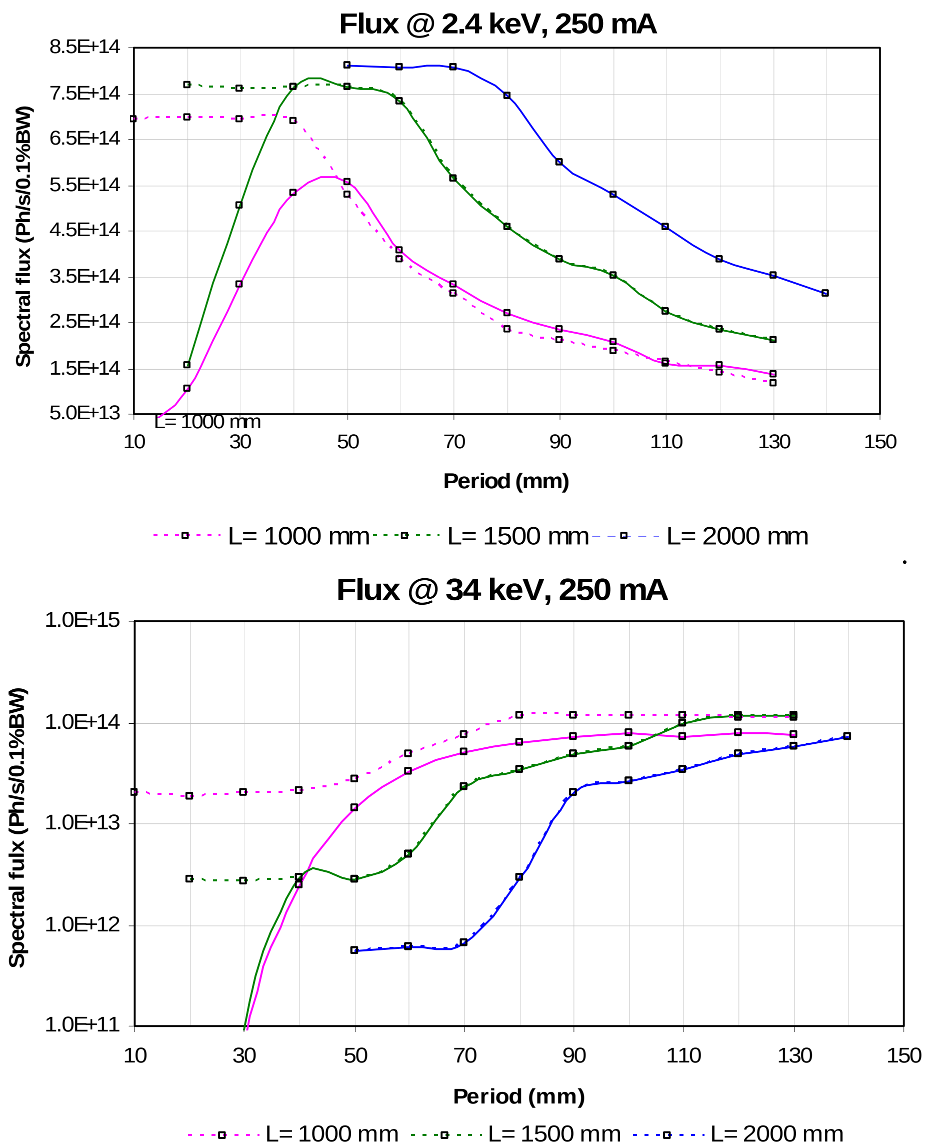

Figure 3. *Flux at 2.4 keV (top) and 34 keV(bottom) for a number of devices for a current of 250 mA. Dashed lines show the performance of a superconducting device. Solid line show the performance of a conventional wiggler with a minimum magnetic gap of 12.5 mm.*

It should be noted that the effect of constraining the insertion device to conventional technology is mainly appreciable at 250 mA. At 400 mA of electron current in the ring, the effect is not so intense, as shown in Figure 4.

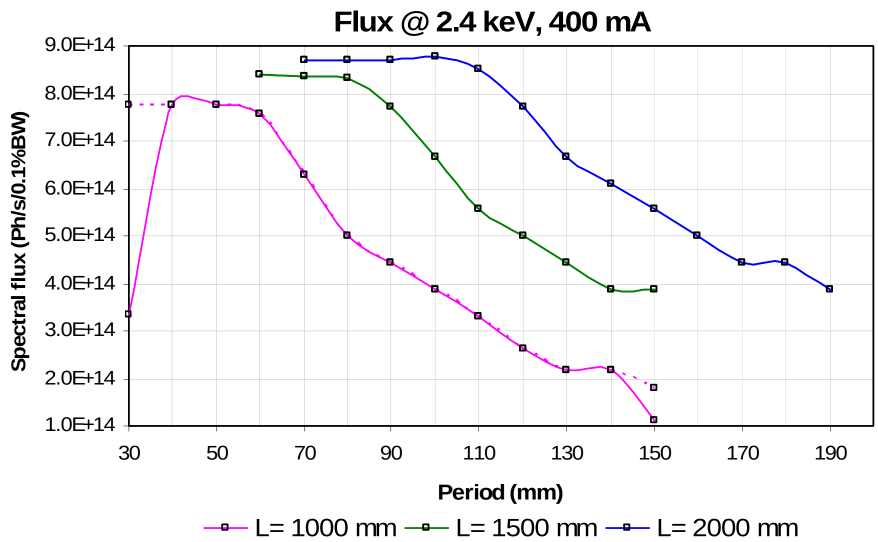

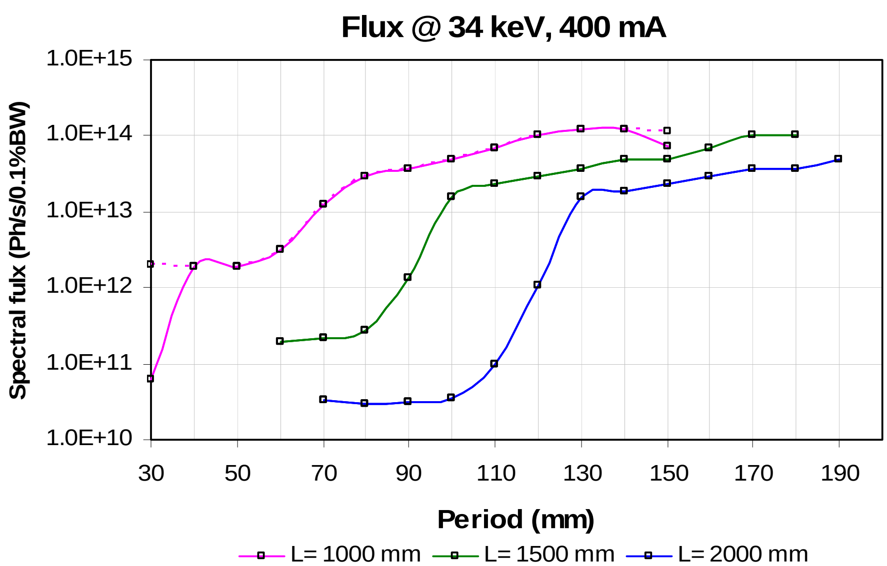

Figure 4. *Flux at 2.4 keV (top) and 34 keV(bottom) for a number of devices for a current of 400 mA. Dashed lines show the performance of a superconducting device. Solid line show the performance of a conventional wiggler with a minimum magnetic gap of 12.5 mm.*

In any case, the constraint of using conventional technology does not introduce changes in Table 6.

4.2. maximum length

There are two main criteria to limit the length of the devices. The first one is the space availability in the accelerator straight sections. The other is the cost of the devices: shorter the device, cheaper it is.

With respect to the first, it has been advised from Experiments Division to leave enough free space in the straight section to leave open the possibility of placing two IDs. The medium straight section available length –flange to flange– is 3.21 m. To leave open the possibility of installing 2 IDs in the same straight, the maximum length allowed is 1.605 m for each device. This gives a maximum magnetic length of ~1.0 m per device (300 + 300 mm left at each side for correctors, BPMs, space for magic fingers, etc). This constraint is also pushing –along with the demand of maximum flux at high energies– towards a short device of ~1 m long. The drawback is that at high energies and with a current of 250 mA, the maximum flux that can be reached at high energies will be $7.5 \cdot 10^{13}$ Ph/s/0.1%BW, lower than the maximum achievable for 1.5 m long device, which is $1.2 \cdot 10^{14}$ Ph/s/0.1%BW.

4.3. New results

In order to explore the limits of the performance of the device, we have considered the scenario of having 100 mA of current in the ring. This is shown in Table 7 below.

Length 1000 mm, current 100 mA													
Period (mm)	10	20	30	40	50	60	70	80	90	100	110	120	130
Number of periods N	100	50	33	25	20	16	14	12	11	10	9	8	7
H Slit (mrad)	1.5	1.5	1.5	1.5	1.5	1.5	1.5	1.5	1.5	1.5	1.5	1.5	1.5
Power through slit 0-7 keV (W)	434.3	429.4	332.6	230.8	175.8	135.2	118.1	101.2	92.7	84.2	75.8	67.3	58.9
Power through slit 7-20 keV (W)	700.1	700.2	700	584.7	480.1	388.8	340.3	291.8	267.5	243.2	218.9	194.6	170.3
Power through slit 20-INF keV (W)	416.8	415.5	560.4	700	700	656.7	578	497.2	457	416.2	375.1	333.8	292.3
Power through slit 7 - INF (W)	1117	1116	1260	1285	1180	1046	918	789	725	659	594	528	463
Power through slit 0-20 keV (W)	1134	1130	1033	816	656	524	458	393	360	327	295	262	229
Power through slit (W)	1551	1545	1593	1516	1356	1181	1036	890	817	744	670	596	522
K maximum (total power)	1.792	3.581	5.965	9.344	12.819	16.605	19.372	22.139	24.907	27.674	30.442	33.209	35.977
K	1.792	3.581	5.965	9.344	12.819	16.605	19.372	22.139	24.907	27.674	30.442	33.209	35.977
Flux @ 2.4 keV (Ph/s/0.1%BW)	3.95E14	3.88E14	2.80E14	1.87E14	1.41E14	1.07E14	1.57E14	1.34E14	1.23E14	1.11E14	1.00E14	8.90E13	7.78E13
Flux @ 34 keV (Ph/s/0.1%BW)	6.86E13	6.83E13	9.47E13	1.17E14	1.14E14	1.04E14	1.48E14	1.28E14	1.18E14	1.08E14	9.74E13	8.67E13	7.60E13

Table 7*. Photon fluxes at low and high energies (green cells) and maximum K values (yellow cells) for a number of wigglers 1 m long and a number of periods. Blue cells mark the limiting constraint.*

The performance of the device is shown in Figure 5. It should be noted that, not taking into account the technology, the limit in the flux at high periods comes from the total power delivered to Front End.

The effect of considering the conventional technology has also not really a big impact on the performance, at least for periods above 80 mm. At low energies, the decrease in the flux is negligible, and at high energies the spectral photon flux is reduced from $1{\cdot}10^{14}$ to $3{\cdot}10^{13}$.

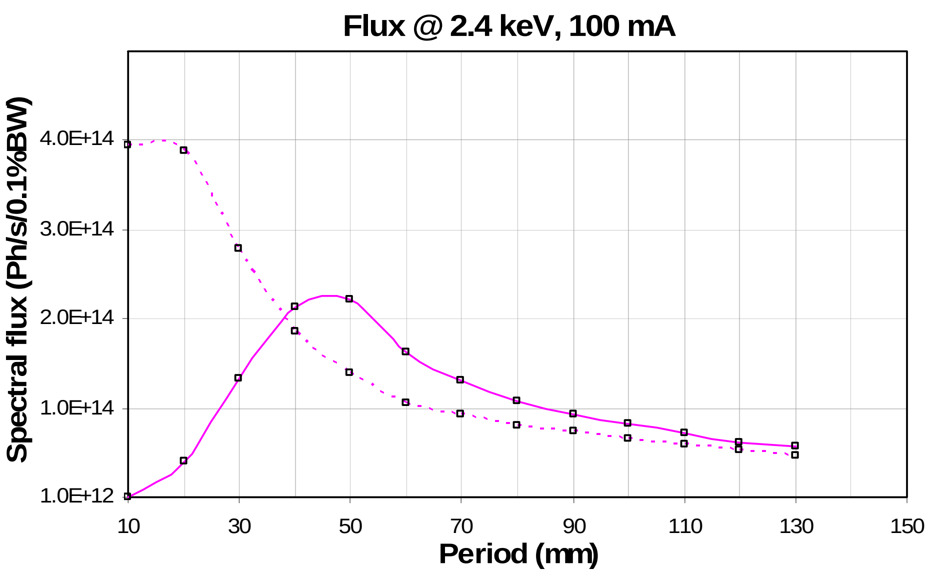

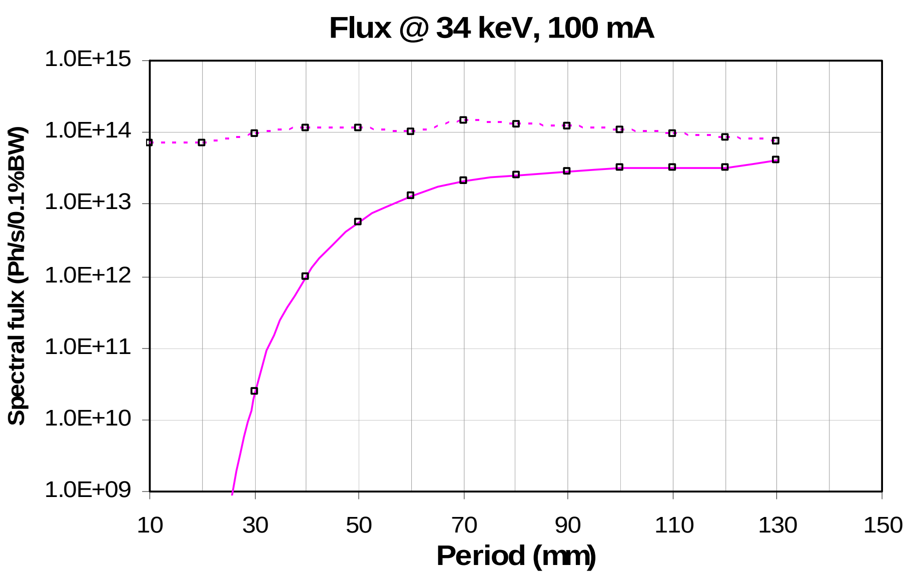

Figure 5. *Flux at 2.4 keV (top) and 34 keV(bottom) for a number of devices for a current of 100 mA. Dashed lines show the performance of a superconducting device. Solid line show the performance of a conventional wiggler with a minimum magnetic gap of 12.5 mm.*

5. Ripple in the lower part of the spectrum

The last constraint to be taken into account is the ripple in the lower part of the spectrum. This ripple appears when low-K devices are considered. It comes from the superposition of undulator-like light. According to Experiments Division, the ripple should be avoided as much as possible, and the maximum tolerated level is 3.4% (this limit can be relaxed to 7% - 8% if necessary, taking into account that simulations carried out are considering perfect insertion devices, without phase error.

In Figure 6 we present the ripple noise for a 1 m device, for different period lengths. Different current scenarios have been also taken into account.

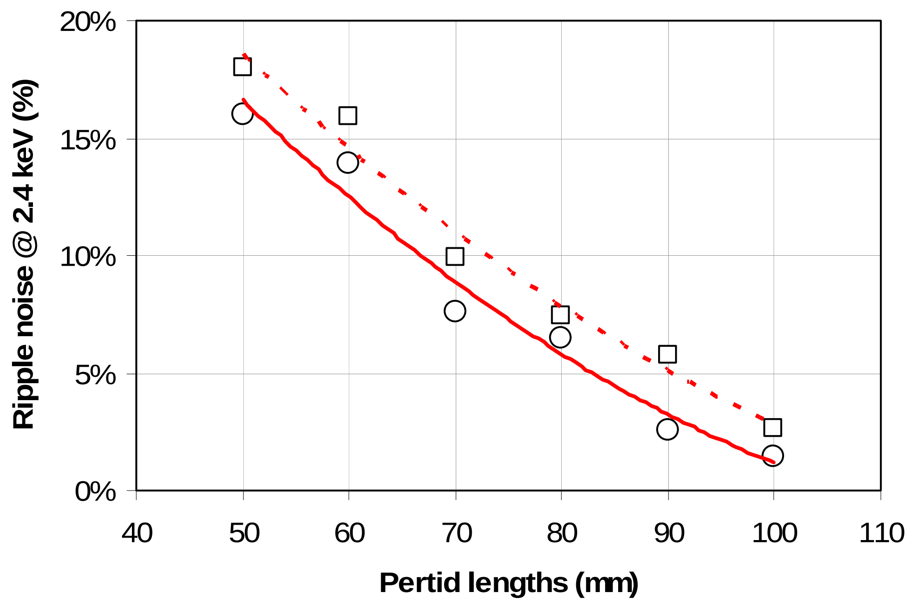

Figure 6. *Ripple noise in the lower part of the spectrum for a wiggler of 1 m long. Dashed line corresponds to the case of 400 mA and solid line to the scenario of 250 and 100 mA in the accelerator.*

As shown in Figure 6, the worst scenario is 400 mA. The reason for is that in this scenario, the K values should be reduced in order no to overpass the limitation in power delivered to monochromator. So, lowering K value has the consequence of increasing the ripple.

6. Selection of main parameters

According to the above results and discussions, we propose the following parmeters for the wiggler to feed the EXAFS beamline:

Magnitude	Value
Magnetic length of the device	1 m
Period length	80 mm
K value at 100 mA	12.976
K value at 250 mA	12.976
K value at 400 mA	9.328
Ripple noise at 400 mA	7.4%
Ripple noise at 100, 250 mA	6.5%
Flux @ 2.4 keV – 100 mA	$1.08 \cdot 10^{14}$
Flux @ 2.4 keV – 250 mA	$2.69 \cdot 10^{14}$
Flux @ 2.4 keV – 400 mA	$5.01 \cdot 10^{14}$
Flux @ 9.0 keV – 100 mA	$1.41 \cdot 10^{14}$
Flux @ 9.0 keV – 250 mA	$3.53 \cdot 10^{14}$
Flux @ 9.0 keV – 400 mA	$4.84 \cdot 10^{14}$
Flux @ 34 keV – 100 mA	$2.49 \cdot 10^{13}$
Flux @ 34 keV – 250 mA	$6.24 \cdot 10^{13}$
Flux @ 34 keV – 400 mA	$2.89 \cdot 10^{13}$